CrossMark

J. Fluid Mech. (2016), *vol.* 807, *pp.* 205–220. © Cambridge University Press 2016
doi:10.1017/jfm.2016.608

The interaction of a rising bubble and a particle in oscillating fluid

D. V. Lyubimov[1], L. S. Klimenko[2], T. P. Lyubimova[2,†] and L. O. Filippov[3]

[1]Perm State University, Perm 614990, Russia

[2]Institute of Continuous Media Mechanics UB RAS, Perm 614013, Russia

[3]Universite de Lorraine, Nancy 54000, France

(Received 6 June 2015; revised 11 August 2016; accepted 15 September 2016;
first published online 18 October 2016)

This article considers the interaction of a rising bubble and a sedimenting fine particle in an incompressible viscous liquid under vibrations (ultrasound). The particle is subject to Stokes, Basset and buoyancy forces, and average force due to the inhomogeneity of the pulsating field. It is shown that the main contribution to the average force is made by interference of the external field and the field caused by the monopole mode of bubble oscillations. The interaction force is the attraction of the particle to the bubble. It is found that even weak vibrations lead to considerable increase of the effective cross-section of particle capture by the bubble. The evaluation of the efficiency of the flotation process exposed to an ultrasound action is discussed.

Key words: bubble dynamics, particle/fluid flow

1. Introduction

Particle–bubble interactions are known to play an important role in many technological and physical processes, including acoustic coagulation, supersonic techniques in medicine, and flotation. Flotation is an energy-efficient and eco-friendly process, which is applied in almost all sectors of the economy. Every year, more than 2 billion tonnes of raw material are enriched and approximately 100 billion cubic metres of industrial wastewater are purified using flotation technology. Therefore, improvement of the efficiency of flotation is a high priority. One of the current tendencies in the intensification of mass transfer processes, including flotation, is based on ultrasound exposure (Zaidi 1997; Aldrich & Feng 1999; Ozkan 2002; Gogate, Tayal & Pandit 2006; Wenze, Haixin & Jun 2008; Filippov *et al.* 2013).

In flotation theory, the bubble–particle interaction can hardly be modelled without referring to the hydrodynamic approach. However, existing theories of the flotation process are either of empirical nature (Gaudin 1957; Dobby & Finch 1987) or do not account for the action of the external fields (Nguyen 1999; Phan *et al.* 2003).

The behaviour of inclusions (gas bubbles, liquid drops or solid particles) in oscillating liquid has long attracted interest from the viewpoint of average forces acting on inclusions. If the oscillations are caused by acoustic waves, these forces are

† Email address for correspondence: lubimova@psu.ru

https://doi.org/10.1017/jfm.2016.608 Published online by Cambridge University Press

called acoustic radiation forces, or acoustic radiation pressure. It is generally agreed to divide the acoustic radiation forces into two types, namely primary forces, which represent direct acoustic wave action on inclusions, and secondary forces, which are related to the action of acoustic waves, scattered on the inclusions (Doinikov 2003).

The first study on the radiation force (primary) acting on a spherical particle in a plane sound wave was made by King (1934). An extension of this work considering an incident spherical wave was provided by Embleton (1954). It was found that the particle can be either attracted to or repulsed by the source of sound depending on their relative distance. The effect of particle compressibility on the radiation force was investigated theoretically and experimentally by Yosioka & Kawasima (1955). They showed that small bubbles with eigenfrequencies less than the imposed ones are collected at the nodes, whereas large bubbles are collected at the antinodes.

A general expression for the radiation force acting on a rigid particle in non-viscous fluid can be found in Gorkov (1962). This author assumed that the particle radius is much smaller than the acoustic wavelength; additionally, his expression is valid only for plane waves. Later, Nyborg (1967) also considered the radiation force exerted by a spherical wave on a rigid sphere. He showed that the travelling part of the spherical wave can be described by Gor'kov theory by adding a correction term. The effect of compressibility for arbitrary shape of the acoustic wave was taken into account in Alexeev (1983) and Krasil'nikov & Krylov (1984). The force acting on deformable inclusions in uniform pulsating flow of non-viscous fluid was calculated in Lyubimov, Lyubimova & Cherepanov (2002).

Recent studies (Doinikov 1994; Danilov & Mironov 2000; Settnes & Bruus 2012) have advanced the theoretical treatment by introducing thermoviscous effects for both incident ultrasound waves and the scattered wave from a particle.

The secondary radiation force was studied for the first time in Bjerknes (1906), where the expression for the interaction force of two bubbles, the so-called Bjerknes force, was obtained. Konig (1891) was the first to derive an analytical expression for the interaction force of two rigid spheres in a non-viscous fluid.

The first expression for the interaction force of a pulsating gas bubble and an oscillating spherical particle was obtained by Bjerknes (1915). He considered the motions of the particle and the bubble to be independent of each other and the surrounding liquid far from the bubble and particle as quiescent. This restriction was removed much later in Alexeev (1991), but the expression obtained in this work is applicable only for large distances between the particle and the bubble (much larger than their sizes). Doinikov & Zavtrak (1996) obtained an expression for the interaction force valid for any distance, but they took into account only monopole oscillations of the bubble, which, as will be shown below, are not sufficient.

This paper describes a theoretical model for bubble–particle interaction in a liquid under external vibrations. The host liquid is assumed to be incompressible and the gravitational field is taken into account. Analysis of different components of the pulsating field scattered on the bubble allows estimation of their contributions to the radiation force acting on the particle. The trajectories of the particle motion near a pulsating bubble are calculated. The evaluation of the efficiency of the flotation process exposed to an ultrasound action is discussed.

The paper is organized as follows. Section 2 is devoted to the problem statement, where the real physical task is described. In § 3, the vibration-induced flow around the bubble and the particle is considered. In § 4, we calculate the average motion of the particle and the bubble, and find the trajectories of the particle and the effective cross-sections of particle capture by the bubble. Section 5 provides some final conclusions.

https://doi.org/10.1017/jfm.2016.608 Published online by Cambridge University Press

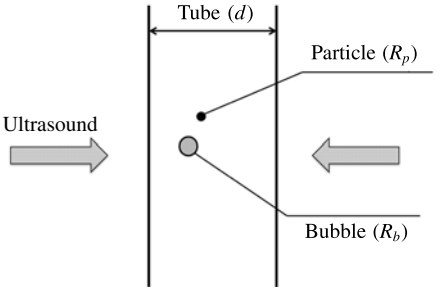


FIGURE 1. Scheme of the set-up.

2. Problem statement

Let us investigate the behaviour of a solid heavy particle in the vicinity of a gas bubble rising in an incompressible viscous liquid filling a long cylindrical vertical tube of diameter d which is much larger than the bubble and particle sizes, i.e. $d \gg R_b \gg R_p$ (where R_b and R_p are the bubble and particle radii). The system is subjected to a gravity field and an external vibrational (ultrasound) field. The ultrasound waves propagate in the direction perpendicular to the tube axis; that is why in the modelling we consider horizontal vibrations, namely standing waves. The system is sketched in figure 1.

The presence of two significantly different time scales – the pulsation time $1/\omega$ and the dissipative time $2R_b/u$ (where u is the rising velocity of the bubble) – makes it reasonable to consider the 'fast' (or pulsating) and 'slow' (or average) motions separately.

3. Pulsating motion

In this section, we consider the vibration-induced flow around the bubble and particle. We focus on the case when the particle is much smaller than the bubble, which allows neglect of the flow induced by the wave scattered on the particle. Let us consider the pulsating flow around a gas bubble suspended in a liquid filling the entire space.

We adopt the following assumptions for the problem.

(1) The vibration frequency is so high that the thickness of the Stokes boundary layer $\delta = \sqrt{2\nu/\omega}$ (where ν is the kinematic viscosity of the liquid) is much smaller than the bubble and particle radii.
(2) The sound wavelength at the vibration frequency is at least one order larger than the tube radius, $\lambda \gg d$.
(3) The amplitude of vibration b is small compared with the particle radius, $b \ll R_p$.
(4) The deviation of the bubble surface from a spherical shape is small compared with the bubble radius, which leads to the restriction $bd \ll R_b^2$.

These assumptions permit us to describe a pulsating flow around the bubble using the inviscid fluid model (assumption 1) and to consider the imposed vibration field as spatially uniform (assumption 2). Under assumptions 3 and 4, we can linearize the Euler equation for the pulsating velocity field near the bubble. The ranges of the parameter values of practical interest are presented in table 1 (where f is the vibration frequency) and are consistent with the assumptions made.

https://doi.org/10.1017/jfm.2016.608 Published online by Cambridge University Press

R_p, μm	R_b, μm	b, μm	f, kHz	d, cm
<50	500–1000	10	10–20	1

TABLE 1. Reference values of real system parameters.

The pulsating velocity field includes the imposed field $\boldsymbol{U}_{vib}$ and the scattered fields of the liquid velocity cased by the monopole $\boldsymbol{U}_m$ and translational $\boldsymbol{U}_{tr}$ bubble motions:

$$\boldsymbol{U} = \boldsymbol{U}_{vib} + \boldsymbol{U}_m + \boldsymbol{U}_{tr}. \tag{3.1}$$

Here, $\boldsymbol{U}_{vib} = b\omega \boldsymbol{i} \cos \omega t$ is the velocity of the oscillatory flow at a sufficient distance from the bubble and $\boldsymbol{i}$ is the direction of vibrations.

3.1. *Monopole motion*

Let us first consider the liquid motion due to the monopole or radial bubble motion, which is induced by the term representing pressure forcing, $q\mathrm{e}^{\mathrm{i}\omega t}$. Using the linearized Euler equation and the continuity equation for the liquid velocity in the spherical coordinate system, one can find by simple integration that the pressure and velocity amplitudes of the liquid near the bubble are as follows:

$$U_m = \frac{c_1}{r^2}, \tag{3.2a}$$

$$p = \mathrm{i}\omega\rho \frac{c_1}{r} + q, \tag{3.2b}$$

where r is the radial distance from the bubble centre and the unknown constant c_1 is related to the surface deviation ζ through the kinematic condition

$$\mathrm{i}\omega\zeta = \frac{c_1}{R_b^2}. \tag{3.3}$$

Another boundary condition is the normal stress balance condition, which in terms of gas pressure variation, p_g', reads

$$p - p_g' = \frac{2\gamma}{{R_b}^2}\zeta. \tag{3.4}$$

We assume that the gas behaves polytropically, so that $p_g V^k = \text{const}$. Substitution of the pressure in a liquid ((3.2), taking into account (3.3)) in the normal stress balance condition (3.4) gives the expression for the surface deviation,

$$\zeta = \frac{q}{\omega^2\rho R_b - \dfrac{3kp_0}{R_b} + \dfrac{2\gamma}{{R_b}^2}}. \tag{3.5}$$

Neglecting the surface tension, we come to the expression for the natural frequency,

$$\omega_0^2 = \frac{3p_0 k}{\rho {R_b}^2}, \tag{3.6}$$

https://doi.org/10.1017/jfm.2016.608 Published online by Cambridge University Press

which coincides with the result obtained in Plesset & Prosperetti (1977) and Leighton (2012). Thus, the expression (3.5) can be written in a more compact form,

$$\zeta = \frac{q}{\rho R_b(\omega^2 - \omega_0^2)}. \tag{3.7}$$

Substituting (3.7) in (3.2), we obtain the following expressions for the velocity and pressure of monopole motion:

$$\boldsymbol{U}_m = \left(\frac{\mathrm{i}\omega\, qR_b}{(\omega^2 - \omega_0^2)\rho}\frac{1}{r^3}\right)\boldsymbol{r}\mathrm{e}^{\mathrm{i}\omega t}, \tag{3.8a}$$

$$p_m = \left(-\frac{\omega^2 qR_b}{\omega^2 - \omega_0^2}\frac{1}{r} + q\right)\mathrm{e}^{\mathrm{i}\omega t}, \tag{3.8b}$$

where $\boldsymbol{r}$ is a radial vector along the radial coordinate r.

The pressure q far from the bubble can be determined by the following reasoning. Under the assumption that the sound wavelength at the vibration frequency is much larger than the tube diameter, the far-field pressure is found from the Euler equation in the form

$$q\mathrm{e}^{\mathrm{i}\omega t} = -\mathrm{i}\omega\rho(\boldsymbol{U}_{vib}\cdot\boldsymbol{r}_b), \tag{3.9}$$

where $\boldsymbol{r}_b$ is the radius vector of the bubble centre which is counted from the pressure nodes. The coordinates of the nodes are determined by the type of generation of oscillations in the liquid. We suppose that the oscillations in the liquid are generated in such a way that the pressure node is located in the tube centre. Under the assumption that the sound wavelength at the vibration frequency is much larger than the tube diameter, the acoustic wave inside the liquid is spatially uniform; thus, the action of the ultrasound can be described as the vibrations of the tube walls.

3.2. *Translational motion*

For the study of the translational motion of the bubble it is convenient to write the equations and boundary conditions describing the dynamics of the system in the reference frame moving with the bubble centre. In this case, we assume that the bubble motion is one-dimensional, and the direction of this motion coincides with the direction of the vibration axis $\boldsymbol{i}$ ($U_b\boldsymbol{i}$ is the velocity of the centre of mass of the bubble relative to the laboratory reference frame). In this reference frame, for a fluid of density ρ the Euler and continuity equations may be written as

$$\frac{\partial \boldsymbol{v}}{\partial t} = -\frac{\nabla p}{\rho} - \frac{\mathrm{d}U_b}{\mathrm{d}t}\boldsymbol{i}, \tag{3.10a}$$

$$\nabla\cdot\boldsymbol{v} = 0. \tag{3.10b}$$

Far from the bubble, its effect on the fluid flow becomes insignificant; hence, the fluid velocity matches the vibration velocity, i.e.

$$\boldsymbol{v}(r\to\infty) = (U_{vib} - U_b)\boldsymbol{i} = (b\omega\cos\omega t - U_b)\boldsymbol{i}. \tag{3.11}$$

On the bubble surface ($r = R_b$), the kinematic condition and the normal stress balance condition are satisfied:

$$\frac{\partial\zeta}{\partial t} = \boldsymbol{v}\cdot\frac{\boldsymbol{r}}{r}, \tag{3.12a}$$

$$p - p_g = -\gamma K, \tag{3.12b}$$

https://doi.org/10.1017/jfm.2016.608 Published online by Cambridge University Press

where K is the surface curvature, γ is the surface tension coefficient and ζ is the surface deviation, which depends on time and on the polar angle ϑ measured from the direction of vibration. By solving (3.10) with boundary condition far from the bubble (3.11) we obtained the flow fields, which are convenient to write for irrotational flow in terms of a velocity potential and pressure,

$$\varphi = \left(b\omega r + \frac{c_2}{r^2}\right)\cos\vartheta\cos\omega t - U_b r\cos\vartheta, \tag{3.13a}$$

$$p = \rho\omega\left(b\omega r + \frac{c_2}{r^2}\right)\cos\vartheta\sin\omega t. \tag{3.13b}$$

We will now determine the surface deviation. It follows from the kinematic condition (3.12*a*) that $\zeta = c_3\cos\vartheta\cos\omega t$. However, this solution describes the translational oscillations of the bubble as a whole, which is impossible in the reference frame moving with the bubble centre, so it follows that $c_3 = 0$. Thus, in the leading order the bubble surface deviation vanishes.

The unknown constant c_2, as well as the velocity of the bubble centre U_b, can be obtained from boundary conditions on the bubble surface (3.12). Indeed, taking into consideration that the pressure inside the bubble is determined by the mean surface curvature $p_g = \gamma K = 2\gamma/{R_b}^2$, it can be found that $c_2 = -b\omega{R_b}^3$ and $U_b = 3b\omega\cos\omega t$, which coincides with the result obtained in Lyubimov *et al.* (2002). Substituting c_2 and U_b in (3.13), the velocity of the liquid can be written as

$$\boldsymbol{v} = b\omega\left\{\left(-2 + 2\frac{{R_b}^3}{r^3}\right)\cos\vartheta\,\boldsymbol{e}_r + \left(2 + \frac{{R_b}^3}{r^3}\right)\sin\vartheta\,\boldsymbol{e}_\vartheta\right\}\cos\omega t. \tag{3.14}$$

If we come back to the laboratory reference frame and exclude the incident wave from (3.14), the expression for the required liquid velocity caused by the translational bubble motion in the leading order reads

$$\boldsymbol{U}_{tr} = b\omega\left(3\frac{{R_b}^3}{r^5}(\boldsymbol{i}\cdot\boldsymbol{r})\,\boldsymbol{r} - \frac{{R_b}^3}{r^3}\boldsymbol{i}\right)\cos\omega t. \tag{3.15}$$

Finally, the pulsating velocity of the liquid near the gas bubble in the external pulsating field can be written as

$$\boldsymbol{U} = \boldsymbol{U}_{vib} + (\boldsymbol{U}_{vib}\cdot\boldsymbol{r}_b)\frac{\omega^2 R_b}{(\omega^2 - \omega_0^2)}\frac{\boldsymbol{r}}{r^3} - \boldsymbol{U}_{vib}\frac{R_b^3}{r^3} + (\boldsymbol{U}_{vib}\cdot\boldsymbol{r})\frac{3R_b^3}{r^4}\frac{\boldsymbol{r}}{r}. \tag{3.16}$$

4. Average motion

In this section, we calculate the average motion of the particle and the bubble. As the directions of vibrations and gravity are mutually perpendicular, we can separate their influences on the particle motion. The total force exerted on the particle is calculated as the sum of two contributions. The first one originates from the velocity field $\boldsymbol{V}$ caused by the rising motion of the bubble, and is decomposed as the sum of gravity force, viscous drag, Basset force and added mass. The other is the average vibration force $\boldsymbol{F}_{vib}$ originating from the oscillatory velocity field $\boldsymbol{U}$, produced by the incident vibration field plus the monopole and dipole fields scattered by the bubble. For the range of particle sizes under consideration (see table 1), the particle radius is sufficiently small that the Faxen corrections (Faxen 1922) can be neglected. We also

https://doi.org/10.1017/jfm.2016.608 Published online by Cambridge University Press

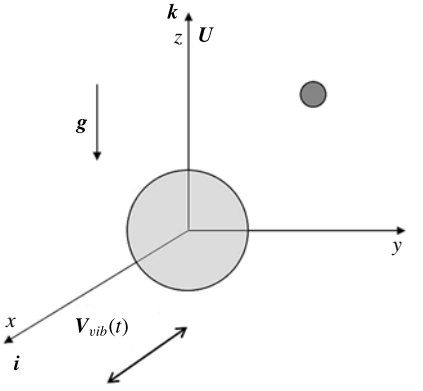


FIGURE 2. Problem configuration.

assume that the bubble rises with constant velocity in laminar flow; thus, the Saffman lift term is zero. Under the above assumptions, the momentum equation for a particle per unit volume in the coordinate system associated with the bubble centre (figure 2) reads

$$\left(\rho_s + \frac{\rho}{2}\right)\frac{\mathrm{d}^2\boldsymbol{r}}{\mathrm{d}t^2} = \boldsymbol{F}_{vib} - \frac{9\eta}{2R_p{}^2}\left(\frac{\mathrm{d}\boldsymbol{r}}{\mathrm{d}t} - \boldsymbol{V}\right) - \frac{9\rho}{2R_p}\sqrt{\frac{\nu}{\pi}}\int_0^t \frac{\mathrm{d}}{\mathrm{d}\zeta}\left(\frac{\mathrm{d}\boldsymbol{r}}{\mathrm{d}\zeta} - \boldsymbol{V}\right)\frac{\mathrm{d}\zeta}{\sqrt{t-\zeta}} + (\rho_s - \rho)\boldsymbol{g}, \tag{4.1}$$

where ρ_s is the particle density, and η and ν are the dynamic and kinematic viscosities of the liquid. Assuming a creeping flow regime, $\boldsymbol{V}$ represents the velocity field caused by the rising bubble, if it were not oscillating, which according to Landau & Lufshits (1987) is given by

$$\boldsymbol{V} = \frac{uR_b}{2r}\left[\frac{\boldsymbol{r}}{r^2}(\boldsymbol{k}\cdot\boldsymbol{r}) + \boldsymbol{k}\right] - u\boldsymbol{k}, \tag{4.2}$$

where $\boldsymbol{k}$ is the unit vector in the vertical direction and the velocity of the rising bubble is

$$u = gR_b^2/9\nu. \tag{4.3}$$

In deriving (4.1) we neglected the rectified diffusion, which can be reasonable, as discussed in the Appendix. We consider that the bubble rises maintaining sphericity. According to Levich (1962), the bubble remains in spherical form if its radius is less than the critical radius, namely $R_b < \sqrt{\gamma/\rho g} \approx 3000$ μm. For the range of bubble size under consideration (see table 1) this condition is satisfied.

We did not take into account the Derjaguin–Landau–Verwey–Overbeek (DLVO) forces due to the fact that our calculations became unreliable at distances less than $\times 10^{-2}R_p$ (the thickness of the Stokes boundary layer). As shown in Elimelech *et al.* (1995), the DVLO forces are comparable to the Stokes force at distances less than $\times 10^{-5}R_p$.

The average vibration force, acting on the particle from the oscillating liquid, was found in Lyubimov *et al.* (2002) for the case of incompressible fluid under the assumption that the vibration frequency is high and the amplitude is small.

https://doi.org/10.1017/jfm.2016.608 Published online by Cambridge University Press

These authors considered the general case of non-uniform inviscid pulsating flow and solved the equation of liquid motion in terms of potential, assuming that the particle size is small compared with the spatial scale of the pulsating field inhomogeneity. In the laboratory reference frame after averaging over the vibration period, the expression for the average force $\boldsymbol{F}_{vib}$ per unit volume was obtained in the form

$$\boldsymbol{F}_{vib} = \frac{3}{4}\rho \frac{\rho_s - \rho}{\rho_s + \frac{1}{2}\rho} \nabla \overline{U^2}. \tag{4.4}$$

This expression can also be obtained from the general expression for the acoustic radiation force in inviscid liquid, derived in Krasil'nikov & Krylov (1984), assuming that the liquid is incompressible. In the work of Settnes & Bruus (2012), the analytical expression for the acoustic radiation force was extended to the case of viscous liquid. This expression is valid for any particle radius and boundary-layer thickness provided that both of these length scales are much smaller than the wavelength of the ultrasound wave. These authors considered separately generation by standing and travelling waves. For inviscid incompressible liquid and a standing wave, their expression for the radiation force is reduced to the ones obtained in previous works, namely (4.4). They also showed that in the case of inviscid ambient liquid, a travelling planar wave has no influence on average particle motion. For a travelling planar wave, the radiation force is proportional to the boundary-layer thickness; thus, in inviscid liquid this force is equal to zero. Despite the good agreement with other works in the limiting cases, the radiation force obtained by Settnes & Bruus (2012) does not describe the change from attraction to repulsion at small distances from the particle; this change was found experimentally (Klotsa *et al.* 2007, 2009) and numerically (Lyubimova, Lyubimov & Shardin 2011; Lyubimov, Baydin & Lyubimova 2013).

The vector field of this force is plotted in figure 3(*a*), where the vibrations are applied in the horizontal direction. As can be seen, all over the domain the vibrational force is directed towards the bubble surface; thus, it is reasonable to expect that particles will be attracted to the bubble.

It can be shown that at large distances from the bubble, the most essential contribution to the average force is due to the interference of the external vibration field and the field scattered by the bubble, which means that consideration of only monopole oscillations of the bubble (as, for example, in Doinikov & Zavtrak 1996) would be inadequate.

Indeed, we need to evaluate the dependence of $\boldsymbol{F}_{vib}$ on the distance from the bubble surface. We restart from (3.1) and exhibit nearly all contributions to $\overline{U^2}$ one by one ($\overline{U_{vib}^2}$, $\overline{\boldsymbol{U}_{vib}\cdot\boldsymbol{U}_m}$, $\overline{\boldsymbol{U}_{vib}\cdot\boldsymbol{U}_{tr}}$, $\overline{\boldsymbol{U}_m\cdot\boldsymbol{U}_{tr}}$, $\overline{U_m^2}$, and so on) using the full expression (3.16). The first term, $\overline{U_{vib}^2}$, is spatially uniform and does not contribute to the force. The contribution of the solely monopole mode, $\overline{U_m^2}$, decreases with distance as r^{-5}.

Now let us calculate the cross-contribution. The result of averaging the scalar product is written as

$$\overline{\boldsymbol{U}_{vib}\cdot\boldsymbol{U}_m} = \frac{1}{2}\frac{\omega^2 R_b}{(\omega^2-\omega_0^2)}\frac{1}{r^3}(\boldsymbol{U}_{vib}\cdot\boldsymbol{r}_b)(\boldsymbol{U}_{vib}\cdot\boldsymbol{r}). \tag{4.5}$$

Thus, for the cross-component of the velocity squared, we obtain an expression similar to that of the potential dipole field. Moreover, the expression for the contribution of

https://doi.org/10.1017/jfm.2016.608 Published online by Cambridge University Press

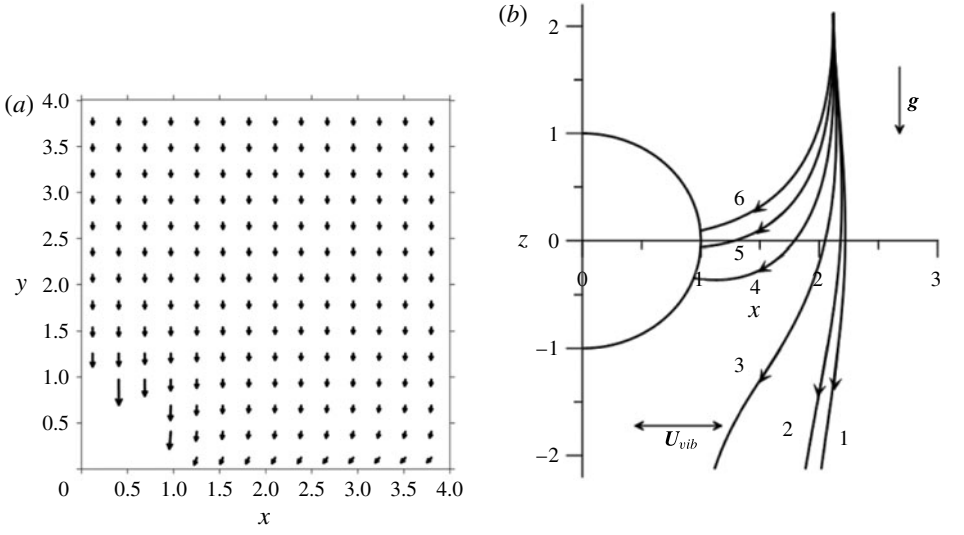


FIGURE 3. (*a*) The vector field of the average vibrational force. (*b*) The trajectories of particle motion for different vibration intensities: 1 – in the absence of vibrations, 2 – $b\omega/u = 1.6$, 3 – $b\omega/u = 1.92$, 4 – $b\omega/u = 3.2$, 5 – $b\omega/u = 4.8$ and 6 – $b\omega/u = 6.4$ ($\gamma = \rho_s/\rho = 8.9$, $R_b = 0.5$ mm, $R_p = 0.02$ mm). The vibrations are directed along the x-axis and the gravitational force is directed along the y-axis.

the cross-component (3.7) to the force $\boldsymbol{F_{cr}}$ is similar to that of the electric field of the dipole, namely

$$\boldsymbol{F}_{cr} \sim \frac{\boldsymbol{U}_{vib}}{r^3} - \frac{3\boldsymbol{r}\cdot\boldsymbol{U}_{vib}}{r^5}\boldsymbol{r}. \tag{4.6}$$

At large distances, this force decreases more slowly than the contributions of the monopole and translational modes to the force, and at distances comparable to the bubble radius all terms are of equal significance.

4.1. *Trajectories of the particle motion*

Equation (3.16) was solved numerically using the Euler method. For each time step, the Basset force was computed from previous time steps using an algorithm for partial differential equations, namely a Caputo-type fractional derivative (Diethelm *et al.* 2005).

The calculations show that in the absence of vibrations, the effect of the bubble on the particle motion becomes insignificant at a distance of approximately one bubble diameter – the particle trajectories are nearly vertical (figure 3*b*, curve 1). When subjected to vibrations, the particle trajectories are gradually distorted, and at a certain value of the vibration parameter the particles hit the bubble surface (figure 3*b*, curves 2–6).

The problem under consideration has some peculiarities. If the initial position of the particle lies in the plane formed by the directions of vibration and gravity, the particle does not leave this plane in its motion, i.e. the particle trajectory is two-dimensional. However, if the initial position of the particle does not belong to this plane, then the trajectory of the particle is three-dimensional (figure 4).

The density ratio also influences the bubble–particle interaction (figure 5*a*,*b*). The trajectories of particles just slightly denser than the liquid are not much different from the streamlines (figure 5*a*, curves 1, 2), which means that vibrations do not

https://doi.org/10.1017/jfm.2016.608 Published online by Cambridge University Press

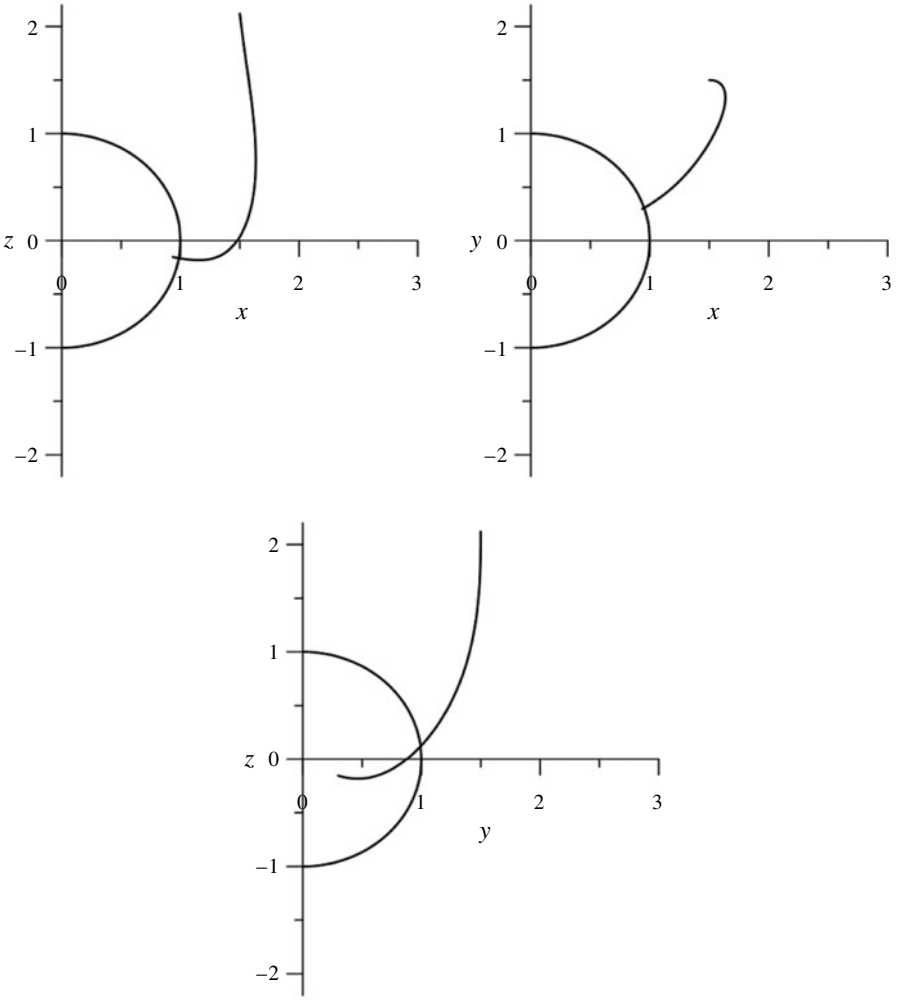


FIGURE 4. The trajectories of the particle motion in three dimensions: $b\omega/u = 3.2$, $\gamma = \rho_s/\rho = 8.9$, $R_b = 0.5$ mm, $R_p = 0.02$ mm, $r_b = 0.5$ mm. The vibrations are directed along the x-axis and the gravitational force is directed along the y-axis.

have sufficient effect on such particles, so that they are carried away from the bubble surface with the flow. If the particle is much denser then the liquid, the gravity force controls the particle behaviour (figure 5*a*, curve 5). However, if we slightly increase the ultrasound intensity, the vibration influence on the particle attraction grows significantly (figure 5*b*); even particles 20 times heavier than the liquid will move to the bubble surface.

4.2. *Collision cross-section*

A quantitative estimation of the vibration effect on the bubble–particle interaction can be made by calculating the efficiency of collision,

$$E_c = \frac{{b_c}^2}{{R_b}^2}, \tag{4.7}$$

https://doi.org/10.1017/jfm.2016.608 Published online by Cambridge University Press

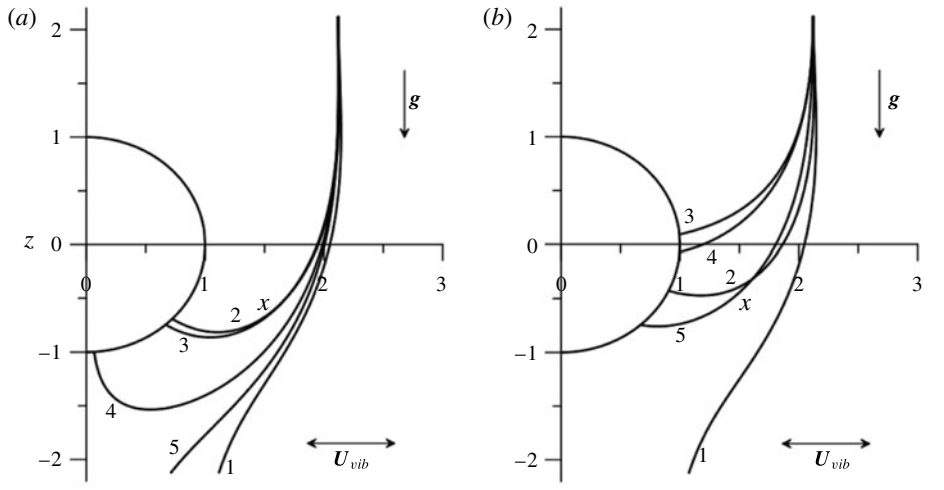


FIGURE 5. The trajectories of the particle motion for different density ratios: (*a*) $b\omega/u = 3.2$, 1 – $\gamma = 2$, 2 – $\gamma = 4$, 3 – $\gamma = 8$, 4 – $\gamma = 16$, 5 – $\gamma = 20$; (*b*) $b\omega/u = 8$, 1 – $\gamma = 1.1$, 2 – $\gamma = 1.2$, 3 – $\gamma = 2$, 4 – $\gamma = 20$ ($\gamma = \rho_s/\rho = 8.9$, $R_b = 0.5$ mm, $R_p = 0.02$ mm, $r_b = 0.5$ mm). The vibrations are directed along the x-axis and the gravitational force is directed along the y-axis.

where b_c is the maximal radius of the flow tube, inside which all particles located inside this tube settle on the bubble surface. In the absence of vibrations the problem has axial symmetry; thus, the flow tube has the same symmetry.

According to the Flint and Howarth theory (Flint & Howarth 1971), one of the most important factors responsible for capturing small particles is gravitational force. The collision efficiency for inertialess particles is defined by

$$E_c = \frac{G}{1+G}, \tag{4.8}$$

where G is the terminal settling velocity of the particles in the undisturbed fluid, namely

$$G = \frac{u_g}{u} = \frac{2}{9}\left(\frac{\rho_s}{\rho} - 1\right)\frac{gR_p^2}{\nu} \div \frac{1}{9}\frac{gR_b^2}{\nu} = 2\left(\frac{\rho_s}{\rho} - 1\right)\frac{R_p^2}{R_b^2}. \tag{4.9}$$

According to the assumption that the particle radius is much smaller than the bubble radius, the settling velocity G is much smaller than one ($G \ll 1$), which allows (4.8) to be transformed for the collision efficiency as follows:

$$E_c = \frac{G}{1+G} = G(1 - G + \cdots) \approx G. \tag{4.10}$$

Substitution of this expression in the formula of the collision efficiency (4.7) gives the following expression for the impact distance:

$$\frac{b_c}{R_b} = \sqrt{2\left(\frac{\rho_s}{\rho} - 1\right)}\frac{R_p}{R_b}. \tag{4.11}$$

https://doi.org/10.1017/jfm.2016.608 Published online by Cambridge University Press

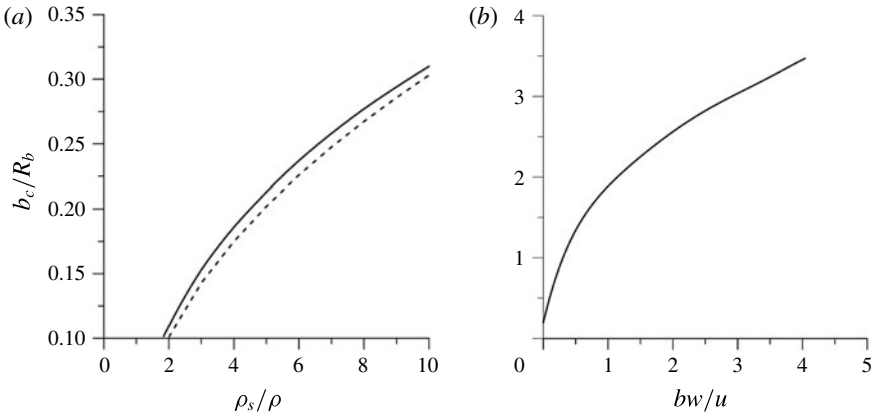


FIGURE 6. (*a*) Impact distance versus density ratio; the dashed line is the impact distance, according to the Flint and Howarth theory. (*b*) Impact distance versus vibration velocity ($\gamma = \rho_s/\rho = 2$, $R_b = 0.5$ mm, $R_p = 0.05$ mm, $r_b = 0.5$ mm).

Our calculations of the momentum equation for a particle (3.16), in the absence of vibrations and inertia of the particle, give the impact distance b_c, which quantitatively agrees with the result obtained by Flint and Howarth (figure 6*a*). To demonstrate the influence of vibration on impact distance, we choose the x-coordinate of the collision cross-section (z is equal to 0) as an impact distance. When subjected to vibrations even of low intensity, the impact distance substantially increases (figure 6*b*).

A full understanding of the vibration effect on the efficiency of collision can be achieved by calculating the collision cross-section. For this, we consider a horizontal plane which is located at a distance from the centre of the bubble that approximately equals its diameter (figure 7*a*). Analysis of the trajectories of the particles passing through this plane allows us to determine the region (collision cross-section) in which the captured particles will approach the bubble surface (figure 7*b*). Normalization of the collision cross-section to that of the bubble leads to an important characteristic in the kinetic theory of flotation: the efficiency of collision. Our calculations, in the absence of vibrations and inertia, give the collision cross-section, which is axially symmetric and quantitatively agrees with the collision efficiency obtained by Flint and Howarth (figure 7*b*, domain 1). When subjected to vibrations even of low intensity, the collision cross-section increases significantly (by several times, figure 7*b*, domain 2), which results in a strong increase in the efficiency of the flotation process as a whole. The collision cross-section is curiously roughly circular (figure 7*b*, domain 2). This form of the collision cross-section is related to the fact that for chosen parameter values, the radial motion of the bubble is dominant. If we consider a bubble located closer to the pressure node, the form of the collision cross-section (figure 8*a*) changes, and for a bubble in the pressure node, for which there is translational bubble motion only, the form of the collision cross-section is not circular any more (figure 8*b*).

5. Conclusion

The interaction of a solid particle with a gas bubble rising in a liquid in the presence of acoustic vibrations was studied. The host liquid was assumed to be incompressible and the gravitational field was taken into account. The particle is

https://doi.org/10.1017/jfm.2016.608 Published online by Cambridge University Press

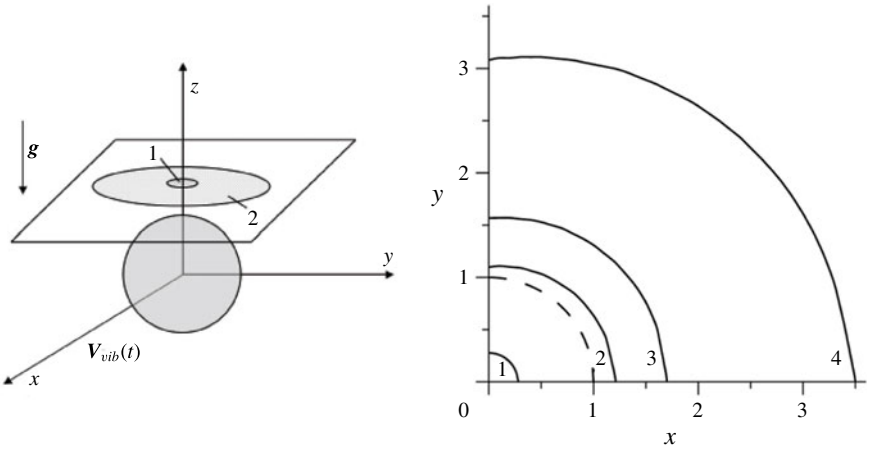


FIGURE 7. Collision cross-section: domain 1 – in the absence of vibrations; domain 2 – in the presence of vibrations, $b\omega/u = 0.4$; domain 3 – $b\omega/u = 0.8$; domain 4 – $b\omega/u = 4$. Here, $\gamma = \rho_s/\rho = 2$, $R_b = 0.5$ mm, $R_p = 0.05$ mm, $r_b = 0.5$ mm. The dashed line is the projection of the cross-section of the bubble.

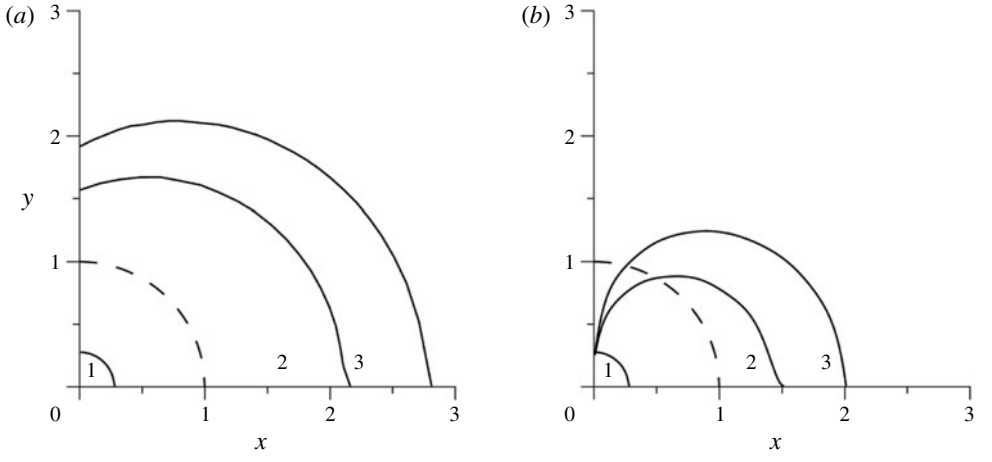


FIGURE 8. Collision cross-section: (*a*) $r_b = 0.1$ mm; (*b*) $r_b = 0$. Domain 1 – in the absence of vibrations; domain 2 – in the presence of vibrations, $b\omega/u = 4$; domain 3 – $b\omega/u = 8$. Here, $\gamma = \rho_s/\rho = 2$, $R_b = 0.5$ mm, $R_p = 0.05$ mm. The dashed line is the projection of the cross-section of the bubble.

subject to Stokes, Basset and buoyancy forces, and the average force due to the inhomogeneity of the pulsating field. A theoretical model including the imposed field and the scattered fields of the monopole and translational motions of the bubble was developed. The model is applicable for the case when the particle size is much smaller than that of the bubble. Analysis of different components of the pulsating field scattered on the bubble allowed us to estimate their contributions to the average force acting on the particle. It was found that consideration of only monopole oscillations of the bubble is not sufficient.

https://doi.org/10.1017/jfm.2016.608 Published online by Cambridge University Press

The trajectories of the particle motion near a pulsating bubble have been determined. It was shown that if the initial position of the particle lies in the plane formed by the direction of vibration and gravity, the particle does not leave this plane in its motion; thus, the particle trajectory is two-dimensional. However, if the initial position of the particle does not belong to this plane, then the trajectory of the particle is three-dimensional.

The results were used for calculations of the collision cross-section – the domain where the particles hit the bubble. We found that even moderate vibrations lead to a multifold increase in the collision cross-section. The results of this study can be used for intensification of flotation processes by applying ultrasound treatment.

Ultrasonic treatment of gas flow in the slurry in flotation apparatus makes it possible to significantly affect the collision processes, which increases the efficiency of the flotation process as a whole.

We would like to remark that interesting behaviour can be found in the case of resonance. To consider this case, one needs to take into account the damping effect. According to Leighton (2012), the damping constant consists of three parts: the thermal damping constant, the viscous damping constant and the radiation damping constant. The first two constants depend strongly on the ratio of the bubble radius to the damping length (the thickness of the viscous or thermal boundary layer), and these constants are important for small values of this ratio. In contrast to this, the radiation damping constant is nearly the same for different bubble sizes. The radiation damping is caused by the liquid compressibility. Thus, to study the resonances in a proper way, small bubbles in compressible liquid should be considered. In our paper, we focus on large enough bubbles, to show that the increase of the collision efficiency is not related to the size effect, as, for example, in Diaz-Penafiel & Dobby (1994). However, in future we plan to extend our analysis to small bubbles; in this case the resonance with damping will be considered.

Acknowledgements

This work was carried out under the framework of the France–Russia programme of scientific collaboration ARCUS and was supported by the Government of the Perm region (under contract N C-26/0004.3), the Russian Foundation for Basic Research (grant 15-01-09069) and the French national programme ICEEL Carnot.

Appendix

Let us show that this is reasonable to neglect a rectified diffusion in our case. According to Hsieh & Plesset (1961), the increase of the bubble radius due to rectified diffusion is $\delta R_b \sim \delta t D\varepsilon^2 c/(3\rho R_b)$, where D is the diffusion coefficient, c is the dissolved concentration and ρ is the gas density. For an air bubble dissolved in water, $Dc/\rho = 4\times10^{-7}$ cm^2 s^{-1}. Another parameter, $\varepsilon = p_{vib}/P_0$, is the ratio of the vibration pressure amplitude to the average pressure in the liquid (atmospheric pressure). The vibration pressure amplitude is related to the pulsating velocity of the liquid by $p_{vib} = \rho\omega d U_{vib} = \rho b\omega^2 d$. For the parameters under consideration, $p_{vib} \approx 2\times10^5$ Pa. We analyse the time interval δt during which the particle is located near the bubble (at a distance of approximately the bubble diameter), $\delta t = 2d_b/u = 12\nu/gR_b \approx 2\times10^{-3}$ s. Then, $\delta R_b \approx 4\times10^{-10}$ m, which is much smaller than the bubble radius. Thus, variation of the bubble radius due to rectified diffusion can be neglected.

https://doi.org/10.1017/jfm.2016.608 Published online by Cambridge University Press

REFERENCES

ALDRICH, C. & FENG, D. 1999 Effect of particle size on flotation performance of complex sulphide ores. *Miner. Engng* **12**, 701–707.

ALEXEEV, V. N. 1983 K voprosy o radiocionnoi sile davleniya zvyka na sfery. *Akust J. AS USSR* **2**, 129–136.

ALEXEEV, V. N. 1991 Sili, deistvyushie mezhdy puzirkom i chasticei v zvukovom pole. *Akust J.* **37**, 597–606.

BJERKNES, C. A. 1915 *Hydrodynamische Fernkrafte*. Englemann, Leipzing.

BJERKNES, V. F. K. 1906 *Field of Force*. Columbia.

DANILOV, S. D. & MIRONOV, M. A. 2000 Mean force on a small sphere in a sound field in a viscous fluid. *J. Acoust. Soc. Am.* **107**, 143–153.

DIAZ-PENAFIEL, P. & DOBBY, G. S. 1994 Kinetic studies in flotation columns: bubble size effect. *Miner. Engng* **7**, 465–478.

DIETHELM, K., FORD, N. J., FREED, A. D. & LUCHKO, Y. 2005 Algorithms for the fractional calculus: a selection of numerical methods. *Comput. Meth. Appl. Mech. Engng* **194**, 743–773.

DOBBY, G. S. & FINCH, J. A. 1987 Particle size dependence in flotation derived from a fundamental model of the capture process. *Intl J. Miner. Process.* **21**, 241–260.

DOINIKOV, A. A. 2003 Acoustic radiation forces: classical theory and recent advances. *Recent Res. Devel. Acoustics* **1**, 39–67.

DOINIKOV, A. A. 1994 Acoustic radiation pressure on a compressible sphere in a viscous fluid. *J. Fluid Mech.* **267**, 1–21.

DOINIKOV, A. A. & ZAVTRAK, S. T. 1996 Interaction force between a bubble and a solid particle in a sound field. *Ultrasonics* **34**, 807–815.

ELIMELECH, M., GREGORY, J., JIA, X. & WILLIAMS, R. A. 1995 *Particle Deposition and Aggregation. Measurement, Modelling and Simulation*, p. 434. Butterworth-Heinemann, Woburn.

EMBLETON, T. F. W. 1954 Mean force on a sphere in a spherical sound field. i. (theoretical). *J. Acoust. Soc. Am.* **26**, 40–45.

FAXEN, H. 1922 Der Widerstand gegen die Bewegung einer starren Kugel in einer zähen Flüssigkeit, die zwischen zwei parallelen ebenen Wänden eingeschlossen ist. *Ann. Phys.* **373**, 89–119.

FILIPPOV, L. O., MATININ, A. S., SAMIGUIN, V. D. & FILIPPOVA, I. V. 2013 Effect of ultrasound on flotation kinetics in the reactor–separator. *J. Phys.: Conf. Ser.* **416**, 012016.

FLINT, R. L. & HOWARTH, W. I. 1971 The collision efficiency of small particles with spherical air bubbles. *Chem. Engng Sci.* **26**, 1155.

GAUDIN, A. M. 1957 *Flotation*, p. 573. McGraw-Hill.

GOGATE, P. R., TAYAL, R. K. & PANDIT, A. B. 2006 Cavitation: a technology on the horizon. *Curr. Sci.* **91**, 35–46.

GORKOV, L. P. 1962 On the forces acting on a small particle in an acoustical field in an ideal fluid. *Sov. Phys. Dokl.* **6**, 773–775.

HSIEH, D. & PLESSET, M. S. 1961 Theory of rectified diffusion of mass into gas bubbles. *J. Acoust. Soc. Am.* **33**, 206–215.

KING, L. V. 1934 On the acoustic radiation pressure on spheres. *Proc. R. Soc. Lond.* A **147**, 212–240.

KLOTSA, D., SWIFT, M. R., BOWLEY, R. M. & KING, P. J. 2007 Interaction of spheres in oscillatory fluid flows. *Phys. Rev.* E **76**, 056314.

KLOTSA, D., SWIFT, M. R., BOWLEY, R. M. & KING, P. J. 2009 Chain formation of spheres in oscillatory fluid flows. *Phys. Rev.* E **79**, 021302.

KONIG, W. 1891 Hydrodynamisch–akustische Untersuchungen. *Ann. Phys.* **278**, 353–370.

KRASIL'NIKOV, V. A. & KRYLOV, V. V. 1984 *Vvedenie v Fizicheskuju Akustiku*. M. Nauka.

LANDAU, L. D. & LUFSHITS, E. M. 1987 *Fluid Mechanics – Course of Theoretical Physics*. Butterworth-Heinemann.

LEIGHTON, T. 2012 *The Acoustic Bubble*, p. 633. Academic.

LEVICH, V. G. 1962 *Physicochemical Hydrodynamics*, p. 573. Prentice Hall.

LYUBIMOV, D. V., BAYDIN, A. Y. & LYUBIMOVA, T. P. 2013 Particle dynamics in a fluid under high frequency vibrations of linear polarization. *Microgravity Sci. Technol.* **25**, 121–126.

https://doi.org/10.1017/jfm.2016.608 Published online by Cambridge University Press

LYUBIMOV, D. V., LYUBIMOVA, T. P. & CHEREPANOV, A. A. 2002 Behavior of a drop (bubble) in a non-uniform pulsating flow. *Adv. Space Res.* **29**, 667–672.

LYUBIMOVA, T., LYUBIMOV, D. & SHARDIN, M. 2011 Interaction of rigid cylinders in a low Reynolds number pulsational flow. *Microgravity Sci. Technol.* **23**, 305–309.

NGUYEN, A. V. 1999 Hydrodynamics of liquid flows around air bubbles in flotation: a review. *Intl J. Miner. Process.* **56**, 165–205.

NYBORG, W. L. 1967 Radiation pressure on a small rigid sphere. *J. Acoust. Soc. Am.* **42**, 947–952.

OZKAN, S. G. 2002 Beneficiation of magnesite slimes with ultrasonic treatment. *Miner. Engng* **15**, 99–101.

PHAN, C. M., NGUYEN, A. V., MILLER, J. D., EVANS, G. M. & JAMESON, J. G. 2003 Investigations of bubble–particle interactions. *Intl J. Miner. Process.* **72**, 239–254.

PLESSET, M. S. & PROSPERETTI, A. 1977 Bubble dynamic and cavitation. *Annu. Rev. Fluid Mech.* **9**, 145–185.

SETTNES, M. & BRUUS, H. 2012 Forces acting on a small particle in an acoustical field in a viscous fluid. *Phys. Rev.* E **85**, 016327.

WENZE, K., HAIXIN, X. & JUN, H. 2008 Study of the effect of ultrasonic treatment on the surface composition and the flotation performance of high-sulfur coal. *Fuel Process. Technol.* **89**, 1337–1344.

YOSIOKA, K. & KAWASIMA, Y. 1955 Acoustic radiation pressure on a compressible sphere. *Acustica* **5**, 167–173.

ZAIDI, S. A. H. 1997 Application of sonic energy to caustic cleaning of coals. *Fuel Process. Technol.* **53**, 31–39.

https://doi.org/10.1017/jfm.2016.608 Published online by Cambridge University Press